

Theodore Yaotsu Wu · John Kao · Jin E. Zhang

A unified intrinsic functional expansion theory for solitary waves

Received: 18 October 2004 / Accepted: 5 December 2004 / Published online: 12 February 2005
© Springer-Verlag 2005

Abstract A new theory is developed here for evaluating solitary waves on water, with results of high accuracy uniformly valid for waves of all heights, from the highest wave with a corner crest of 120° down to very low ones of diminishing height. Solutions are sought for the Euler model by employing a unified expansion of the logarithmic hodograph in terms of a set of intrinsic component functions analytically determined to represent all the intrinsic properties of the wave entity from the wave crest to its outskirts. The unknown coefficients in the expansion are determined by minimization of the mean-square error of the solution, with the minimization optimized so as to take as few terms as needed to attain results as high in accuracy as attainable. In this regard, Stokes's formula, $F^2\mu\pi = \tan\mu\pi$, relating the wave speed (the Froude number F) and the logarithmic decrement μ of its wave field in the outskirt, is generalized to establish a new criterion requiring (for minimizing solution error) the functional expansion to contain a finite power series in M terms of Stokes's basic term (singular in μ), such that $2M\mu$ is just somewhat beyond unity, i.e. $2M\mu \simeq 1$. This fundamental criterion is fully validated by solutions for waves

of various amplitude-to-water depth ratio $\alpha = a/h$, especially about $\alpha \simeq 0.01$, at which $M = 10$ by the criterion. In this pursuit, the class of dwarf solitary waves, defined for waves with $\alpha \leq 0.01$, is discovered as a group of problems more challenging than even the highest wave. For the highest wave, a new solution is determined here to give the maximum height $\alpha_{hst} = 0.8331990$, and speed $F_{hst} = 1.290890$, accurate to the last significant figure, which seems to be a new record.

Keywords Solitary waves on water · Unified intrinsic functional expansion theory · Exact solutions · High-accuracy computation of waves of arbitrary height · Mass and energy transfer

1 Introduction

Theory of solitary waves on water has a long colorful history. It has been enriched by contributions of great significance from pioneering masters and their followers. Strong interests, however, have been largely devoted to the highest and almost highest waves for their full resolution, leaving the very low waves virtually unattended. The fully extended scope of our recent studies is aimed at exposition of the real richness of this wave phenomenon.

In its founding era, Sir George G. Stokes made two contributions of basic importance to its theoretical foundation. In one of them, the behavior of solitary waves attenuating with distance in their outskirts was explored, on linear theory, by Stokes [1] to attain a formula relating the wave speed and the logarithmic flow decrement (see Eq. 2), a relation which Stokes claimed *exact*. The other contribution of Stokes's (1880) examines the crest of the maximum wave, concluding that if a wave should peak to a ridge, it must be a corner of 120°. These milestone marks have left a fundamental impact on subsequent advances in the field.

Serious attempts to calculate steep solitary waves have been developed along a few different approaches, all involving lengthy techniques. One approach adopts various series expansions in powers of a small parameter, usually the wave height

Dedicated to Zhemín Zhèng for celebration of his Eightieth Anniversary

It gives us a great pleasure to dedicate this study to Prof. Zhemín Zhèng and join our distinguished colleagues and friends for the jubilant celebration of his Eightieth Anniversary. Warmest tribute is due from us, as from many others unlimited by borders and boundaries, for his contributions of great significance to science, engineering science and engineering, his tremendous influence as a source of inspiration and unerring guide to countless workers in the field, his admirable leadership in fostering the Institute of Mechanics of world renown, as well as for his untiring endeavor in promoting international interaction and cooperation between academies of various nations.

T.Y. Wu (✉)

California Institute of Technology, Pasadena, CA 91125, U.S.A.
Fellow, Institute of Mechanics, Chinese Academy of Sciences,
Beijing 100080, China
E-mail: tywu@its.caltech.edu

J. Kao

Warner Brothers, Glendale, CA 91203, U.S.A.

J.E. Zhang

The university of Hong Kong, Pokfulam Road, Hong Kong SAR, China

or a certain alternative, for a perturbation scheme that dates back to the pioneering works of [2–4], which, as being the leading order in the expansion, hold only for waves of small amplitude. Higher orders of approximation have been developed numerically to ninth order by [5] and further extended to fourteenth order by [6], and more recently developed in exact form to the fifteenth order by [7]. The extreme waves, including the highest and almost-highest, are difficult to reach by such methods of perturbation expansion due to the singular behavior arising with increasingly large curvature at the crest in the limiting stretch.

In another approach, the method of computation employs certain derived integral equation for computing the wave profile and its speed (for a review, see [8–11]). Various integral equations have been derived and applied by [12–16] and others. A proof of the existence of solitary waves is given by [17] based on their integral equation for sufficiently small wave heights. Here again, difficulties are invariably encountered when the wave approaches its maximum limit.

In still another approach, some boundary-integral formula involving Green's function is adopted for representing analytical functions (such as Cauchy's integral theorem) for computation of wave form and its speed, such as those developed by [7, 18, 19] for steep solitary waves very close to the maximum with very high accuracy. These methods, however, have not been shown applicable to very low waves, such as the earthquake-produced tsunamis progressing in the open ocean, which is of great importance to coastal hazard and safeguard.

In particular, the highest solitary wave has been singled out for investigation by various authors as a special interest by itself. To this topic, contributions have been made by [20–22] (for a review, see [9]). Further advances have been made by more recent contributions, including [7], [10], [23], [24] and others. Accurate solutions are of value to studies on their stability characteristics, which are in turn related to the issue of breaking of shoaling waves and studies on the distinct types of wave breaking.

The class of the almost-highest solitary waves, perhaps the most perplexing of all the waves for its rich content, is difficult to be determined very accurately. Here, it has been discovered by [25] that many integral properties of a solitary wave, including its speed, mass, momentum, and energy, separately attain a maximum, each at a wave height slightly short of the limiting value. The more recent contributions to theory for the almost-highest waves by [7, 10, 18, 19, 26, 27] have shed more light on the topic. Nevertheless, further simplifications of still lengthy techniques would be of great value to be pursued for further advances.

This study attempts to introduce an entirely new theory by a unified scheme of analysis and computation for evaluation of solitary waves, and to yield results uniformly valid with high accuracy for waves of all heights, all modeled as an irrotational flow of incompressible and inviscid fluid. It is pursued along a new approach, distinct from the others mentioned above, under the guideline to take as few unknown variables as needed to achieve resulting accuracy as high as

attainable in practice. To reach this goal, the primary first step is to carry out a clear expository analysis of the intrinsic wave properties underlying the phenomenon in question to determine the base functions called the intrinsic component (IC)-modes, as explained in §3 under the premise of formulation in §2. These mode functions in various flow domains are then unified and used to constitute an expansion of the complex velocity, or its logarithmic hodograph, with unknown coefficients, called the unified intrinsic functional (UIF)-expansion to represent the solution sought as delineated in §4. The unknown coefficients are solved by minimizing a functional, which is just the mean-square error of the solution satisfying all the basic equations involved, with an interactive optimization by two numerical methods to be presented in §4. The two methods complement each other very well in application jointly to produce results of high accuracy to three classes of solitary waves – the extreme, medium and low waves. Results of relevant integral quantities are presented in §5 to update the records. Some reflections and outlooks are expounded in §6 on the present study for further development.

2 The problem and formulation

The problem is to compute a solitary wave of arbitrary height a , progressing in permanent form at a constant speed c on a layer of water of constant depth h initially at rest, and to yield results with a uniform high accuracy over all wave heights. To this problem, Stokes [1] was the first to explore the behavior of a solitary wave attenuating in its outskirts at a rate which Stokes assumes to be exponential. Adopting the Euler equations for irrotational flow of incompressible and inviscid fluid, a model regarded by Stokes as ideal for evaluating such solitary waves, the wave profile $\eta(x, t)$ and the velocity potential, $\phi(x, y, t)$, which satisfies the Laplace equation, $\phi_{xx} + \phi_{yy} = 0$, will thus assume the functional form in x , y , and time t as

$$\begin{aligned}\eta(x, t) &= a e^{-k|x - ct|}, \\ \phi(x, y, t) &= b e^{-k|x - ct|} \cos k(y + h) \\ &\quad (-h \leq y \leq \eta(x, t))\end{aligned}\quad (1)$$

as $|x| \rightarrow \infty$ in the flow region bounded below by the horizontal bottom at $y = -h$ (at which $\phi_y = \partial\phi/\partial y = 0$) and above by the water surface elevated to $y = \eta(x, t)$ from the rest level at $y = 0$. The linearized boundary conditions on continuity and surface pressure ($= 0$) read

$$\eta_t = \phi_x, \quad \phi_t + g\eta = 0 \quad (y = 0),$$

both of which are satisfied by (1), for arbitrary constant a (or b), provided

$$F^2 \mu \pi = \tan(\mu \pi) \quad (F = c/\sqrt{gh}, \quad \mu \pi = kh), \quad (2)$$

where F is the Froude number and $\mu \pi$ is the index of the wave decay rate. And as a stroke of genius, Stokes claimed this relation exact, signifying that relation (2) holds uniformly

valid for fully nonlinear and fully dispersive solitary waves of all heights. However, no further qualifications are found being brought forth by Stokes concerning this relation.

To proceed for the general consideration, we adopt the wave frame of reference moving with the wave speed c of a left-going solitary wave in which the wave appears stationary in the physical (x, y) -plane with a free stream of velocity c incoming in the x -direction, with the wave bounded above by its free surface at $y = \eta(x)$ and below by the horizontal channel floor at $y = -h$. In terms of the complex variables for this irrotational plane flow,

$$\begin{aligned} z &= x + iy, & f &= \phi + i\psi, & w &= df/dz = u - iv, \\ \omega &= \tau + i\theta = \log(c/w), & \tau &= \log(c/q), \\ \theta &= \arctan(v/u), & q &= (u^2 + v^2)^{1/2}, \end{aligned} \quad (3)$$

the complex coordinate z , complex potential f , complex velocity w and the logarithmic hodograph ω are analytic functions of one another. And the pressure p is given by the Bernoulli equation,

$$\frac{1}{2}(u^2 + v^2) + \frac{1}{\rho} p(x, y) + gy = \frac{1}{2}c^2, \quad (4)$$

ρ being the constant fluid density, g the gravity acceleration.

With the length scaled by h and velocity by c , we have the dimensionless variables:

$$\begin{aligned} \alpha &= a/h, & z_+ &= z/h, & f_+ &= f/ch, \\ w_+ &= w/c, & p_+ &= p/\rho c^2, & q_+ &= q/c, \end{aligned} \quad (5)$$

and have the * omitted henceforth for brevity. The flow domain occupies an infinite strip in the f -plane: $-1 < \psi < 0$, $-\infty < \phi < \infty$, bounded between the free surface at $\psi = 0$ and the channel floor at $\psi = -1$. Taking f as the independent variable, the problem becomes to find the analytic function $w = w(f)$, or $\omega = \omega(f)$, under the boundary conditions:

$$q^2 + \frac{2}{F^2}\eta = 1 \quad (\text{on } \psi = 0), \quad (F = c/\sqrt{gh}), \quad (6)$$

$$\theta = 0 \quad (\text{on } \psi = -1 \text{ and on } \phi = 0), \quad (7)$$

$$\tau + i\theta \rightarrow 0 \quad \text{as } \phi \rightarrow \pm\infty. \quad (8)$$

where (6) is given by (4) under condition that $p = \text{const.} = 0$ on $\psi = 0$, and F is the Froude number characterizing the flow. Condition (7) for $\phi = 0$ indicates the fore-and-aft wave symmetry. Finally, the physical plane is given by quadrature,

$$z(f) = \int \frac{1}{w(f)} df = \int e^{i\theta(f)} df,$$

from which we deduce in particular for $\psi = 0$ on the free surface,

$$x(\phi) + i\eta(\phi) = i\alpha + \int_0^\phi e^{i\theta(\phi)} d\phi, \quad (9)$$

with $x(\phi = 0) = 0$, and $\alpha = \eta(\phi = 0)$, the wave height. Equivalent to condition (6), its gradient along the free surface

(using $dz = \exp(i\theta)ds$, $\partial\phi/\partial s = q = \exp(-\tau)$, $d\eta/ds = \sin\theta$) gives

$$\frac{\partial}{\partial\phi} q^3 = -\frac{3}{F^2} \sin\theta \quad (\text{on } \psi = 0). \quad (10)$$

Thus, solutions can be attained in terms of the conjugate functions $\tau(\phi)$ and $\theta(\phi)$ of $\omega = \tau + i\theta = \omega(f)$ directly under conditions (7), (8) and (10), as a one-parameter family in F . Instead of F , an alternative is what we call the proportional amplitude parameter,

$$\beta \equiv 1 - q_c^2 (= 2\alpha/F^2) \quad (0 < \beta \leq 1), \quad (11)$$

which follows from applying (6) to a round wave crest, at which $\eta = \alpha$ and $w = q_c$, say, giving $q_c^2 + 2\alpha/F^2 = 1$, or (11). It covers the range from $\beta = 0$ for the vanishing wave ($\alpha = 0$) to $\beta = 1$ for the highest wave (with $q_c = 0$), and has the merit that $\alpha(\beta)$ is monotonic over $(0 < \beta \leq 1)$ but $\alpha(F)$ is multi-valued, as will be seen below.¹

3 Analysis and the intrinsic wave properties

To construct exact solutions for solitary waves of arbitrary height, it is essential to find precisely the asymptotic representation of the flow field in the outskirt, especially for very low waves because of their exceedingly vast outstretch with diminishing rates of decay. And it is equally important to determine precisely the asymptotic behavior of the highest wave about its crest. To proceed, we map the flow domain conformally onto the unit circle $|\zeta| \leq 1$ in the parametric ζ -plane by

$$f = -i + \frac{1}{\pi} \log \left(\frac{1 + \sqrt{\zeta}}{1 - \sqrt{\zeta}} \right)^2, \quad (12)$$

in which the log function and $\sqrt{\zeta}$ are uniquely defined with a branch cut along the positive real ζ -axis, so that the wave surface is mapped onto $|\zeta| = 1$ ($0 < \arg \zeta < 2\pi$), the wave crest onto $\zeta = -1$, and the channel floor at $\psi = -1$ mapped onto the upper and lower side of the branch cut along $0 \leq \zeta \leq 1$, reaching the physical infinities (marked by I and J in Fig. 1) at $\zeta = 1 \pm i0$. On the wave surface,

$$\begin{aligned} \zeta &= e^{i\sigma}, & f &= \frac{\pi}{2} \log \cot \left(\frac{\sigma}{4} \right), \\ \omega &= \tau(\sigma) + i\theta(\sigma) \quad (0 < \sigma < 2\pi). \end{aligned} \quad (13)$$

The corresponding boundary conditions (7), (8) and (10) become

¹ The parameter β is related to some similar ones used in the literature designated (in the present notation) as $\omega_1 = 1 - q_c/q_t$, $\omega_2 = 1 - F^2 q_c^2$, and a few others involving the velocity q_c at the crest, velocity q_t at the trough, wave velocity c and linear wave velocity c_0 . In comparison, $\beta = 1 - (q_c/q_t)^2$, and β in addition has the simple relation $\beta = 2\alpha/F^2$ by Bernoulli's law.

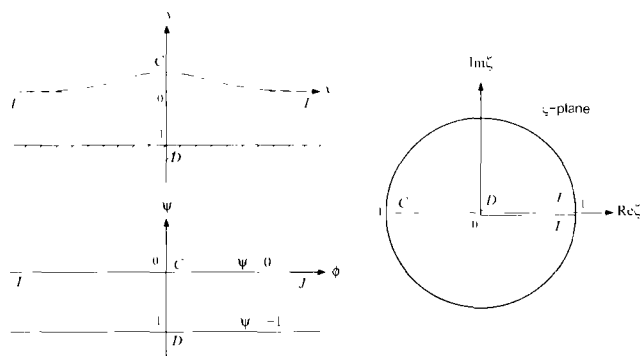


Fig. 1 The conformal maps of the flow domain

$$G(\sigma) \equiv \pi F^2 e^{-3\tau} \sin\left(\frac{\sigma}{2}\right) \frac{\partial \tau}{\partial \sigma} + \sin \theta = 0 (0 < \sigma < 2\pi), \quad (14)$$

$$\theta = 0 \quad (\zeta \text{ real}, -1 < \zeta < 1), \quad (15)$$

$$\omega = \tau + i\theta \rightarrow 0 \quad (\text{as } \zeta \rightarrow 1). \quad (16)$$

This system now affords the solution parametrically in terms of the conjugate functions $\tau(\sigma)$ and $\theta(\sigma)$. Finally, the wave profile is given parametrically by (9), $x = x(\sigma)$, $y = \eta(\sigma)$, where

$$x(\sigma) + i\eta(\sigma) = i\alpha + \frac{1}{\pi} \int_{\sigma}^{\pi} e^{\tau(\sigma) + i\theta(\sigma)} \frac{1}{\sin(\sigma/2)} d\sigma \quad (0 \leq \sigma \leq \pi). \quad (17)$$

The Bernoulli equation (6) on the wave surface now becomes

$$B(\sigma) = e^{-2\tau(\sigma)} - 1 + 2\eta(\sigma)/F^2 = 0 \quad (\eta(\sigma) \text{ by (17)}, 0 \leq \sigma \leq \pi). \quad (18)$$

3.1 Asymptotic free-stream flow field

Near $\zeta = 1$ (the physical infinities), the boundary conditions (14)–(16) on $\omega = \tau(\sigma) + i\theta(\sigma)$ assuming different forms across the point $\zeta = 1$ imply that $\omega(\zeta)$ has a branch-point singularity at $\zeta = 1$. Hence we assume for ω an asymptotic expansion as

$$\omega(\zeta) = \tau + i\theta = \sum_{m=1}^M a_m \{(1 - \zeta)/2\}^{2m\mu} \quad (\text{as } \zeta \rightarrow 1), \quad (19)$$

where μ and a_m 's are real, as yet undetermined, so that $\theta = 0$ for ζ real and $\omega(1) = 0$ to have (15)–(16) satisfied first. That the higher-order terms in (19) assume the successive powers of the leading term is because of the need to balance out the powers and products of τ and θ contained in (14). On the free surface, by (13), we have

$$\tau(\sigma) + i\theta(\sigma) = \sum_{m=1}^M a_m \exp(-i[m\mu(\pi - \sigma)]) \left(\sin \frac{\sigma}{2}\right)^{2m\mu} \quad (0 \leq \sigma \ll \pi).$$

Substituting the above $\tau(\sigma)$ and $\theta(\sigma)$ in (14) and expanding (14) for $0 < \sigma \ll 1$, we find that (14) is satisfied to leading order, for arbitrary a_1 , provided that μ satisfies (2). Thus, the leading term in the series of (19) is Stokes's term, which

has a branch singularity in μ , while μ is the principal-branch root of (2) for assigned $F (> 1, 0 < \mu_1 < 1/2)$ and, as is well accepted, is the only root of (2) that is needed for the solution sought. Finally, to determine M for the length of the finite series in (19), we argue that these M singular terms in (19) must be required to match optimally smoothly with the remaining part of ω that is analytic and regular in the vicinity of $\zeta = 1$, so we propose the following relation,

$$2M\mu \simeq 1, \quad (\text{with } 2M\mu \text{ somewhat greater than unity}), \quad (20)$$

as an ideal criterion for determining $M = M(\mu)$. The general validity of criterion (20) for waves of various heights will be attested later with examples. With this validity so established, the set of (2) and (19)–(20) then provides an optimum asymptotic representation of the singular behavior of $\omega(\zeta)$ in the wave outskirts. Empirically, the set of Eqs. (2) plus (19)–(20) is therefore established as a major generalization of Stokes's original relation (2) to hold in general for solitary waves of all heights.

To have a first assessment of the relationship between $F(\mu)$ and wave height α , we may use Boussinesq-Rayleigh's first-order relation, $F = \sqrt{1 + \alpha}$, so that $\alpha = \tan(\mu\pi)/\mu\pi - 1$, from which μ is found to decrease monotonically from $\mu = 0.371$ (at $\alpha = 1$) down to zero as $\alpha \rightarrow 0$ ($F \rightarrow 1$), as shown in Fig. 2. Thus, criterion (20) gives the value $M(\alpha) = 2, 5, 10, 30$, and 90 at $\alpha = 1, 10^{-1}, 10^{-2}, 10^{-3}$, and 10^{-4} , respectively (see Fig. 2). Such minute solitary waves as $\alpha < 10^{-2}$ may seem unreal, but it is generally known that earthquake-generated tsunami waves progressing in the open Pacific Ocean (of mean depth $h = 4$ km) with a height commonly estimated to be merely $a \simeq 1$ m or less, would give $\alpha = a/h \simeq O(10^{-4})$.

In concluding on this point, we note that while Stokes's relation (2) has invariably been always observed in the literature, it has been employed either as a single factor (i.e. $M = 1$), or in an infinite series of its powers (i.e. $M = \infty$, e.g. [22]), neither bearing the simplicity to avoid lengthy calculations.

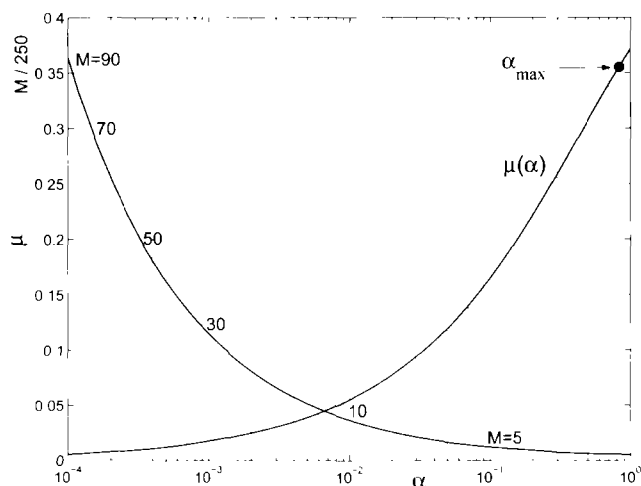


Fig. 2 Variations of $\mu(\alpha)$ and $M(\alpha)$ for solitary waves of all heights (α)

3.2 Asymptotic flow field near the crest of the highest wave

The highest wave with a corner crest of $2\pi/3$ radian ($= 120^\circ$) vertex angle may be regarded as the asymptotic limit of the almost-highest waves to serve for a standard reference. The free stream comes in with a particular Froude number, F_{hst} , say, with the free surface rising to reach a stagnation point at the corner vertex, and falling off symmetrically to downstream infinity. The dimensionless wave height, by (11) with $q_c = 0$, is simply

$$\alpha_{hst} \equiv a_{hst}/h = F_{hst}^2/2, \quad (21)$$

which, as yet undetermined, is the highest of all solitary waves. However, it is well known that F_{hst} is not the maximum Froude number of the fastest solitary wave on water.

Concerning the crest geometry of the highest solitary wave, Stokes [1] made another major contribution by showing, again with an argument in great simplicity, that if a wave should peak to a ridge, it must be a corner of 120° . In addition, Stokes [1] has provided an exact solution for the infinite wedge flow under gravity as

$$f = \phi + i\psi = (2/3F)(e^{i\pi/6}z)^{3/2} \\ (w = df/dz = (1/F)e^{i\pi/4}z^{1/2}), \quad (22)$$

so that $\psi = 0$ and $|w|^2 = |z|/F^2$ (Bernoulli's equation for pressure $p = 0$) on both $\arg z = -\pi/6$ and $= -5\pi/6$, making the two wedge faces free under gravity (acting in the $(-y)$ -direction). As the wedge faces are stationary, this is not a traveling gravity wave. The task that remains is to seek how this exact solution can be adapted (e.g. with or without additional singularities) to describe the leveling off of the wedge faces to fit the highest solitary wave profile.

Reflecting on this issue, we may recall that no inquiries ever appeared in the literature to explore if the primary singularity at the wedge crest should require a secondary singularity to complement the solution structure until Grant [28] did find it to be of a branch type. With this finding, $\omega(\zeta)$ assumes near its corner crest the asymptotic expansion as

$$\omega(\zeta) = -\frac{1}{3} \log\left(\frac{1+\zeta}{2}\right) + \sum_{n=1}^N c_n \left(\frac{1+\zeta}{2}\right)^{2nv} + \omega_r(\zeta) \\ (|\zeta + 1| \ll 1), \quad (23)$$

Here the first term is Stokes's wedge flow solution (22), now adopted to lead the asymptotic expansion about the wave crest (as $\zeta \rightarrow -1$). The added series represents the complementary branch-point singularity at the crest (suggested by Grant [28]) to make the free surface level off from the straight wedge surface and eventually flatten out horizontally with the v and c_n 's real, yet undetermined, so that $\omega(\zeta)$ is real for ζ real to have (15) satisfied. In addition, $\omega_r(\zeta)$ represents the part which is analytic and regular about $\zeta = -1$. The log and branch functions in (23) are uniquely defined with a branch cut from $\zeta = -1$ to $-\infty$.

On the free surface, $\zeta = \exp(i\sigma)$, $0 < \sigma < \pi$, (23) gives $\omega(\sigma) = \tau(\sigma) + i\theta(\sigma)$, where

$$\omega(\sigma) = -\frac{1}{3} \log\left(\cos \frac{\sigma}{2}\right) - i\frac{1}{6}\sigma \\ + \sum_{n=1}^N c_n \exp(inv\sigma) \left(\cos \frac{\sigma}{2}\right)^{2nv} + \omega_r(\sigma).$$

Using the expansion of this $\omega(\sigma)$ about $\zeta = -1$ (or for $0 < \delta \equiv \pi - \sigma \ll 1$), we find that (14) is satisfied up to the first term of the series in (23), for arbitrary c_1 , provided that

$$\sqrt{3}(1+2v) = \tan(v\pi), \quad (24)$$

$$\omega_r(\zeta = -1) = \frac{1}{3} \log\left(\frac{\pi}{3} F_{hst}^2\right). \quad (25)$$

Condition (24) is a transcendental equation with multiple roots, of which the principal root, $v = 0.40134$, is the only one that is needed for much the same reason as for μ of (2). And likewise, the higher terms in (23) assume the consecutive powers of the first to N terms, with the number N determined by an optimization scheme to be described later so as to help render the solution accuracy optimum, though we could also use the empirical relation $2Nv \simeq 1$ as a guideline (like (20) for μ). Condition (25) can be either applied as a constraint on the solution, or reserved for a consistency check on the accuracy of the solution attained.

4 The unified intrinsic functional expansion (UIFE) theory

The foregoing results on the intrinsic behavior of solitary waves in the outskirt and near the highest wave crest will now be incorporated to constitute a unified intrinsic functional expansion (UIFE) theory for solitary waves of all heights. It is based on two principles:

(i) This new theory requires first to establish a unified intrinsic functional (UIF)-expansion for $\omega(\zeta)$ in terms of a set of intrinsic component (IC)-functions (by unifying the above results for the various flow regions) to represent precisely all the intrinsic properties of the wave entity.

(ii) The unknown coefficients in the UIF-expansion for $\omega(\zeta)$ are determined by minimizing the mean-square error E_G^2 of $G(\sigma)$ of (14), or E_B^2 of $B(\sigma)$ of (18), the other conditions (i.e. (15)–(16)) being held as understood, where

$$E_G^2 = \int_0^\pi G^2(\tau(\sigma), \theta(\sigma), \sigma) d\sigma \quad (\text{UIFE-method I}); \quad (26)$$

$$E_B^2 = \int_0^\pi B^2(\tau(\sigma), \eta(\sigma), \sigma) d\sigma \quad (\text{UIFE-method II}). \quad (27)$$

Here, UIFE-method I permits stepwise interactive execution such that the minimization of E_G is optimized stepwise, starting with a few leading terms in the UIF-expansion, with a new term selected in turn by its top ranking among all the competing candidates in making a steep descent in error E_G , the guideline being to find such an expansion with as few terms as needed to achieve a resulting accuracy as high as

attainable in practice. The related UIF-method II employs a numerical code developed here for computation by iteration for convergence to achieve higher accuracies, however with less versatility for optimization. Nevertheless, the two methods complement each other very well; they have been applied jointly in evaluating solitary waves of all heights. In practice, we have found that the Program called 'FindMinimum' of the software Mathematica 5.0 is very well suited for implementing Method-I. Examples are presented below to illustrate their power, simplicity, and high accuracy for solitary waves classified into three regimes: the extreme (comprising the highest and almost highest) waves, medium waves, and low waves.

4.1 The highest solitary wave - by UIF-method I

For the highest solitary wave, occurring with an undetermined Froude number, F_{hst} say, we propose for $\omega(\zeta) = \tau + i\theta$ a unified expansion as follows:

$$\omega = -\frac{1}{3} \left(\log \frac{1+\zeta}{2} + \frac{1-\zeta}{2} \right) + \sum_{m=1}^M \sum_{n=0}^N \{ a_{mn} \left(\frac{1+\zeta}{2} \right)^{2nv} + b_{mn} \zeta^n \} \left(\frac{1-\zeta}{2} \right)^{2m\mu}, \quad (28)$$

where a_{mn} 's and b_{mn} 's are real unknown coefficients so that conditions (15)–(16) are first fulfilled. Here, the first term with the \log function is adopted from Stokes's wedge flow solution (22) to lead the expansion for modeling the cornered wave crest, the second term is added to the first to make the decay rate of their sum one order lower than the first term alone as $\zeta \rightarrow 1$ so as to leave the intrinsic wave properties in the outskirt more intact with the remaining terms. The double series in powers of 2ν unifies the secondary singularity at the crest with the outskirt feature given by the factor $(1-\zeta)^{2m\mu}$. The last series (with coefficients b_{mn}) introduces a function regular everywhere (save at $\zeta = 1$) to admit arbitrary variations of the solution without affecting the outskirt behavior. To this point, we note that an insightful construction of the UIF-expansion such as (28) is actually a primary step of the optimization advocated here.

On the wave surface, $\zeta = \exp(i\sigma)$, we have for $\omega(\sigma) = \tau(\sigma) + i\theta(\sigma)$ ($0 \leq \sigma \leq \pi$),

$$\begin{aligned} \omega(\sigma) = & -\frac{1}{3} \left\{ \log \left(\cos \frac{\sigma}{2} \right) + \left(\sin \frac{\sigma}{2} \right)^2 \right\} \\ & -i \frac{1}{6} (\sigma - \sin \sigma) + \omega_m(\sigma; \mu, \nu), \\ \omega_m(\sigma; \mu, \nu) = & \sum_{m=1}^M \sum_{n=0}^N \left\{ a_{mn} e^{im\nu\sigma} \left(\cos \frac{\sigma}{2} \right)^{2m\nu} + b_{mn} e^{in\sigma} \right\} \\ & \times e^{-im\mu(\pi-\sigma)} \left(\sin \frac{\sigma}{2} \right)^{2m\mu}. \end{aligned} \quad (29)$$

The problem is thus to minimize $E_G^2(a_{mn}, b_{mn})$ of (26) with $\tau(\sigma)$ and $\theta(\sigma)$ given by (29).

For conducting the minimization by principle (ii), we first apply Method-I by employing the Program 'FindMinimum' of the software Mathematica 5.0 which is suitable for serving the present purpose. In short, "FindMinimum[$E[a_{mn}], \{a_{mn}, a_{mn_0}, a_{mn_1}\}$]" (in the Mathematica notation) searches automatically by the program for a local minimum in E as a function of multiple variables in a_{mn} , by finding the path of steepest descent from the given point a_{mn_0} toward a_{mn_1} , and returns, if successful, a list of the form [$E_{min}, \{a_{mn} \rightarrow a^*_{mn}\}$], E_{min} being the minimum value of E found, and a^*_{mn} the value of a_{mn} for which E_{min} is found. However, a local minimum found is not necessarily the overall global one.

In applying Method-I, we start with a few leading terms in (29), and optimize the minimization of E_G stepwise in calculating the unknown coefficients and the unknown parameter μ (or F_{hst} by (2)) in an interactive manner as described, while plotting results in steps for monitoring the progress, the overall global minimum is generally obtained. This is basically the procedure that constitutes the UIF-Method I.

Thus we obtain for the highest solitary wave an accurate solution in terms of (28) with

$$\begin{aligned} E_{min} = & 1.121 \times 10^{-5}; \quad \mu = 0.335056, \quad a_{10} = 0.456569, \\ a_{20} = & -0.102203, \quad a_{30} = -0.158703, \\ a_{40} = & 0.0116986, \quad a_{11} = 0.253853, \quad a_{12} = 0.13121, \\ a_{13} = & 0.0225912, \quad a_{14} = -0.0077326, \\ b_{11} = & -0.329156, \quad b_{12} = -0.0162222, \quad b_{13} = 0.00144751, \\ b_{14} = & 0.0000421358; \\ \alpha_{hst} = & 0.833121, \quad F_{hst} = 1.29083, \quad \beta = 2\alpha/F^2 = 1. \end{aligned} \quad (30)$$

where E_{min} is the minimum root-mean-square error E_G found with the corresponding values of a_{mn} and b_{mn} listed in (30), giving for the highest solitary wave the maximum height $\alpha_{hst} = 0.83312$, with the wave velocity at Froude number $F_{hst} = \sqrt{2\alpha_{hst}} = 1.29083$, accurate, implied by the E_{min} value, at least to four significant figures. Regarding the stepwise descent in error distribution resulting with optimization, the final result for the local error $G(\sigma)$ is plotted over $0 < \sigma < \pi$ in Fig. 3a to exemplify that the resulting small local error is indeed quite uniformly distributed within the bounds of $\pm 2 \times 10^{-5}$.

The problem of the highest wave has also been solved by applying Method-II, which will be presented in §4.5. It is however of interest to cite its result for comparison here. With employing fifteen intrinsic modes, the corresponding result by Method-II reads:

$$\alpha_{hst} = 0.8331990, \quad F_{hst} = 1.2908904, \quad \text{local error} \leq 2 \times 10^{-7}. \quad (31)$$

By comparison with (30) the Method-I result is confirmed for its accuracy as claimed.

Here, we note that the solution so attained is found, interestingly, to consist of four intrinsic component (IC) modes in each of the three groups, namely, in a_{m0} with $M = 4$, and in a_{1n} , b_{1n} , both with $N = 4$. This distribution attained with optimization is a strong indication of the overall real intrinsic

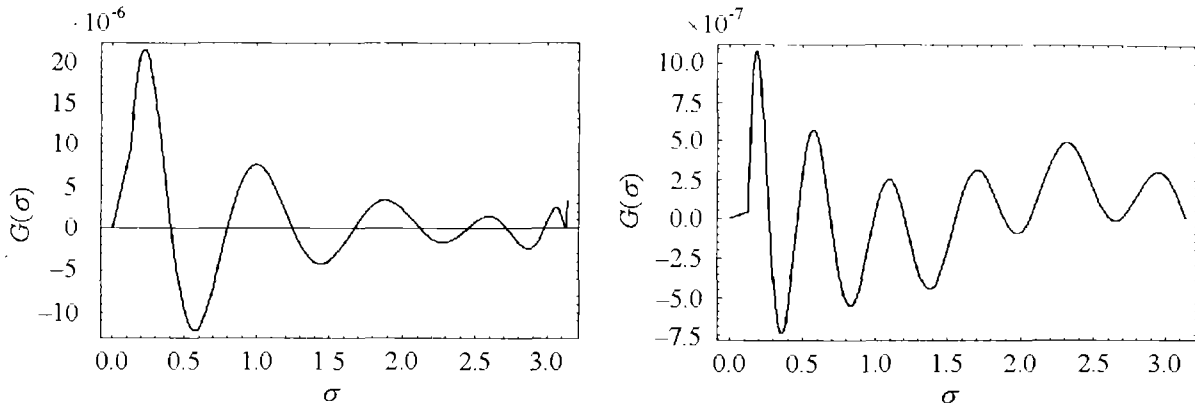


Fig. 3 The local error distribution $G(\sigma) \forall \sigma \in [0, \pi]$ for (a) the highest solitary wave of speed F_{hst} (on the left); (b) for the medium solitary wave of speed $F = 1.20$

nature of the wave entity, which is at considerable variance with the previous solutions in the literature on this problem. (For instance, M is taken in almost all the relevant works as $M = 1$ for one term only in a_{m0} , or else $M = \infty$, e.g. [22]. Likewise, $N = 1$ when the terms in a_{1n} are taken at all.) And with the present distribution, it takes only twelve IC-modes of the functional expansion to achieve an exact solution with a high accuracy to four decimal places by Method-I, and with fifteen IC modes to six decimal places by Method-II. (The solution may be regarded as exact with the resulting $G(\sigma)$ of (14) representing a corresponding ambient pressure, $p_0(\sigma)$, which is as small as, or smaller than that shown in Fig. 3a for its surface gradient.) Finally, we note that with μ found in (30) with $M = 4$, we have $2M\mu = 2.68$, which is about twice that given by criterion (20) in this case. To this end, the solution (28) with the coefficients given by (30) is readily available for applications.

For comparison, we note that the following numerical values have been obtained for the maximum height α_{hst} : 0.827 ([6,20,21]; in review by [9]), 0.8332 ([22,29]), 0.833200 ([23], calculated with 80 terms of the solution series and estimated by extrapolation to 0.833197), and 0.833224 ([24,30]), of which Williams' result is probably the most accurate (to five decimal places). In comparison, our result with $\alpha_{hst} = 0.8331990$ by Method-II is accurate to six decimal places.

4.2 Medium solitary waves - by UIF-method I

The regime of medium solitary waves is defined by the range of $1.10 < F < 1.28$, corresponding crudely to wave height in $0.2 < \alpha < 0.68$ (or $0.25 < \alpha/\alpha_{hst} < 0.8$). Based on the above exposition of the wave properties, we assume for ω its UIF-expansion as:

$$\omega(\zeta) = \tau + i\theta = \sum_{m=1}^M \sum_{n=0}^N \left\{ a_{mn} \left(\frac{1+\zeta}{2} \right)^n + b_{mn} \zeta^n \right\} \times \left(\frac{1-\zeta}{2} \right)^{2mp} \quad (32)$$

with μ given by (2) for assigned F . This expression simply follows from (28) by removing all the terms pertaining to the singularities characterizing the highest wave corner crest, and hence also by setting $2\nu = 1$ in (28). On the free surface, by (13) and (29), we have

$$\tau(\sigma) + i\theta(\sigma) = \omega_m(\sigma; \mu, \nu = 1/2) \quad (\omega_m(\sigma; \mu, \nu) \text{ given in (29)}). \quad (33)$$

This intrinsic functional expansion is found proper to represent the medium and low waves. The problem here is to minimize E_G^2 of (26) with $\tau(\sigma)$ and $\theta(\sigma)$ of (33).

By applying UIF Method-I as delineated in the foregoing, numerical results are obtained for the following representative cases, starting with that for $F = 1.20$, about midway in the regime.

Example 1-2 - $F = 1.20$ ($\mu = 0.295635$). For this case, the final result reads

$$\begin{aligned} a_{10} &= 1.33004, \quad a_{20} = 0.231827, \quad a_{30} = -0.420372, \\ a_{40} &= -0.637748, \quad a_{11} = -1.01148, \\ a_{12} &= 0.226451, \quad a_{13} = -0.007756, \quad a_{14} = 0.0036456, \\ a_{15} &= -0.000876, \quad a_{16} = 0.000672, \\ a_{17} &= -0.00023, \quad a_{18} = 0.000112, \quad a_{21} = -0.466368, \\ a_{22} &= -0.028524, \quad a_{31} = -0.060235; \end{aligned}$$

$$\begin{aligned} \alpha &= 0.457102; \quad E_{rc} \equiv E_{min}/|a_{10}| = 6.66 \times 10^{-7}; \\ \beta &= 2\alpha/F^2 = 0.634864, \end{aligned} \quad (34)$$

which, with the same notation as started for (30), gives the wave height $\alpha = 0.457102$ at Froude number $F = 1.20$, with the maximum relative error E_{rc} , and with the corresponding value of $\beta = 0.634864$. By definition, E_{rc} is the ratio of E_{min} to the largest $|a_{mn}|$ found. This local error distribution $G(\sigma)$, as shown in fig. 3b, appears to conform well with that shown in fig. 3a for the highest wave to lie within the bound of $\pm 1.0 \times 10^{-6}$.

In addition, this case is also computed for comparison by applying UIF-method-II, which uses $\beta (= 2\alpha/F^2)$ as its parameter. With β given in (34), we obtain a solution by

Method-II for $\omega(\zeta)$ from which we deduce for F and α the following result:

$$F = 1.19996681, \quad \alpha = 0.45706371, \\ \text{local error} \leq 1.58 \times 10^{-7} \quad (\text{by UIFE-II}).$$

Thus, with this mutual validation of the two methods, our results in this case demonstrate again that when the intrinsic component functions are well unified, and their terms well optimized in minimizing the solution error, accurate solutions are attained, accurate to the sixth decimal place in this case with taking only fifteen IC-modes of the series.

Very similar results have been obtained for some other medium waves in this regime, as illustrated by two more examples given below. For brevity, their corresponding solutions by method-II, with agreement very similar with the above two cases, will be omitted.

Example I-3 – $F = 1.15$ ($\mu = 0.265724$). For this case, we have the following result:

$$\begin{aligned} E_{min} &= 2.342 \times 10^{-6}; \quad a_{10} = 1.6532, \\ a_{20} &= -0.274723, \quad a_{30} = -0.94692, \\ a_{40} &= -0.0860717, \quad a_{11} = -1.35186, \\ a_{12} &= 0.194478, \quad a_{13} = -0.0004484, \\ a_{21} &= -0.0484815, \quad a_{31} = 0.15268 \\ a_{32} &= 0.0001207; \\ \alpha &= 0.329909; \quad E_{rc} \equiv E_{min}/|a_{10}| = 1.4169 \times 10^{-6}; \\ \beta &= 2\alpha/F^2 = 0.498917, \end{aligned} \quad (35)$$

Example I-4 – $F = 1.10$ ($\mu = 0.225741$). For this case, our result reads:

$$\begin{aligned} a_{10} &= -0.0143334, \quad a_{20} = -0.581676, \\ a_{30} &= 0.612436, \quad a_{40} = 0.193391, \\ a_{50} &= 0.0064854, \quad a_{11} = 0.392035, \\ a_{12} &= 0.0307538, \quad a_{13} = 0.00314869, \\ a_{21} &= 0.195019, \quad a_{22} = 0.0016658, \\ a_{23} &= 0.0159643, \quad a_{24} = 0.00001025 \\ a_{31} &= 0.009254, \quad a_{32} = -0.0138427, \quad a_{41} = 0.0148491, \\ a_{42} &= 0.0245534; \\ \alpha &= 0.212467; \quad E_{rc} \equiv E_{min}/|a_{30}| = 3.497 \times 10^{-6}; \\ \beta &= 2\alpha/F^2 = 0.351185, \end{aligned} \quad (36)$$

In Example I-3, the fact that the solution is represented with a small number of only ten IC-modes is actually a result from neglecting several neighboring modes whose coefficients are of order 10^{-7} or even smaller, while keeping the significant accuracy intact. Here, it further illustrates how effective the optimization scheme can possibly accomplish. In general, using relatively small number of the IC-functions is found sufficient to attain solutions of high accuracy comparable with that given in example I-2. We continue to examine this trend for even lower waves as we shall pursue next.

4.3 Low solitary waves - by UIFE-method I

The range of low and very low solitary waves is designated by their height less than $\alpha = 0.2$ (or $\alpha/\alpha_{hst} < 0.25$). In this regime, the wave decay index μ is small, decreasing monotonically to zero with decreasing wave height (see Fig. 2). From the solution structure (32) we expect, by criterion (20), that increasingly more M terms with coefficients a_{m0} would be needed (see Fig. 2) to achieve solutions of high accuracy. It is of interest to examine the outcome from the present optimized evaluation as illustrated by the following examples. Other than this respect, the unified intrinsic functional structure (32) that has fittingly represented medium waves is found also appropriate to continue representing low waves.

Example I-5 – $F = 1.05$ ($\mu = 0.166553$). For this case, the result reads:

$$\begin{aligned} E_{min} &= 1.249 \times 10^{-6}; \quad a_{10} = 0.2703349, \\ a_{20} &= -0.270266, \quad a_{30} = 0.287217, \\ a_{40} &= -0.184282, \quad a_{11} = -0.0016486, \\ a_{12} &= -0.0021693, \quad a_{13} = -0.00002488, \\ a_{21} &= -0.0665164, \quad a_{22} = 0.0006883, \quad a_{31} = 0.0089701, \\ a_{41} &= 2.3644 \times 10^{-6}; \\ \alpha &= 0.102629; \quad E_{rc} \equiv E_{min}/|a_{30}| = 4.35 \times 10^{-6}; \\ \beta &= 2\alpha/F^2 = 0.186175, \end{aligned} \quad (37)$$

Example I-6 – $F = 1.025$ ($\mu = 0.120442$). For this case, we obtain:

$$\begin{aligned} E_{min} &= 8.343 \times 10^{-7}; \quad a_{10} = 0.642079, \\ a_{20} &= -0.178635, \quad a_{30} = 0.117544, \\ a_{40} &= 0.0379963, \quad a_{50} = -0.536801, \\ a_{60} &= -0.0234055, \quad a_{70} = -0.0069011, \\ a_{80} &= 2.75 \times 10^{-6}, \quad a_{11} = -0.492772, \\ a_{12} &= 0.0003776, \quad a_{21} = -0.011734; \\ \alpha &= 0.0517742; \quad E_{rc} \equiv E_{min}/|a_{10}| = 1.30 \times 10^{-6}; \\ \beta &= 2\alpha/F^2 = 0.0985589, \end{aligned} \quad (38)$$

Example I-7 – $F = 1.005$ ($\mu = 0.054873$). For this case, we have:

$$\begin{aligned} a_{10} &= 0.0342629, \quad a_{20} = -0.0401226, \\ a_{30} &= 0.0218187, \quad a_{40} = -0.0033137, \\ a_{50} &= -0.0018522, \quad a_{60} = 0.00046252, \\ a_{70} &= 0.00032881, \quad a_{80} = 0.000116193, \\ a_{90} &= -0.0002101, \quad a_{10,0} = -0.000073, \\ a_{11,0} &= 0.000061, \quad a_{11} = -0.00002122; \\ \alpha &= 0.0114426; \quad E_{rc} \equiv E_{min}/|a_{20}| = 6.78 \times 10^{-7}; \\ \beta &= 2\alpha/F^2 = 0.022658, \end{aligned} \quad (39)$$

From the above three examples of low waves of height $\alpha = 0.1$, $\alpha = 0.052$, $\alpha = 0.011$, we see that increasingly more IC-functions with a_{m0} in ($m = 1, 2, \dots, M$) are required, as guided by the optimization process, whilst only

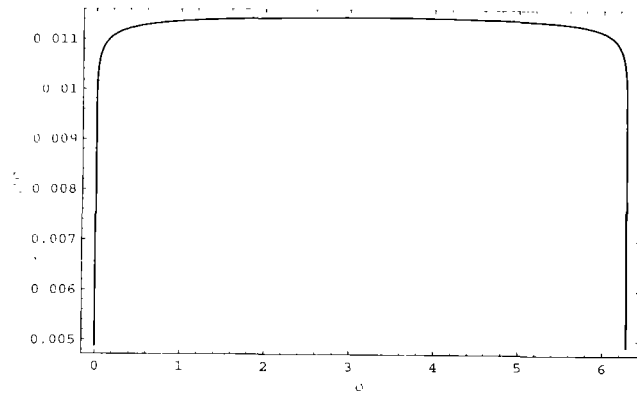


Fig. 4 Wave profile $\eta(\sigma)$ as a function of σ for low solitary wave of speed $F = 1.005$ and amplitude $\alpha = 0.011$ exhibiting steep rise of $\eta(\sigma)$ near $\sigma = 0$ and 2π

a very few terms with a_{mn} in ($n \geq 1$) are needed for attaining solutions of high accuracy. Here, in Example I-6, coefficient a_{80} (of order 10^{-6}) is being retained to exemplify similar cases of their insignificance that their omission would leave the accuracy intact. Thus, we have $M = 4, 7$, and 11 , respectively, giving $2M\mu = 1.332, 1.605, 1.207$. (all being just above unity), an excellent attestation to the validity of the proposed criterion (20). In this connection, the need of taking more M terms for lower waves can be seen in Fig. 4 exhibiting the increasingly steep rise of $\eta(\sigma)$ in an ever narrowing strip adjacent to $\sigma = 0$ and 2π , immediately followed by increasingly sharper turn into an ever flatter mid stretch, with decreasing values of μ . In contrast, for $F = 1.005$, the higher a_{mn} ($n \geq 1$) IC-modes need only one, namely a_{11} to reach jointly with the a_{m0} 's a relative error of $O(10^{-7})$.

We now return to consider the regime of extreme solitary waves, a regime of considerable complexities and richness in new features.

4.4 Extreme solitary waves - by UIFE-method I

Advances in theory and computation of solitary waves of extreme amplitude have been made by recent literatures on the subject, as briefly reviewed earlier. Generally speaking, computations of rather large scale involving a large number of terms in some series expansion or integral equations are required to obtain solutions of quite high accuracy. It is therefore of interest to see how these problems can be resolved by the present new approach. We attempt to demonstrate this trend of such endeavor first by the following case study.

Example I-8 - $F = 1.25$ ($\mu = 0.319173$). By the Method-I procedure, we obtain

$$\begin{aligned} E_{min} &= 6.23 \times 10^{-5}; \quad a_{10} = 5.51911, \quad a_{20} = 9.83542, \\ a_{30} &= -9.74828, \quad a_{40} = -4.77891, \\ a_{50} &= -0.16352, \quad a_{11} = -4.8731, \quad a_{12} = -1.10708, \\ a_{13} &= 0.814336, \quad a_{14} = 0.823774, \\ a_{15} &= -1.08285, \quad a_{16} = 1.07807, \quad a_{17} = -0.843973, \\ a_{18} &= 0.376088, \quad a_{1,10} = -0.09609, \end{aligned}$$

$$\begin{aligned} a_{1,12} &= 0.0434562, \quad a_{1,14} = -0.0222988, \\ a_{1,16} &= 0.0082484, \quad a_{1,18} = -0.00207028, \\ a_{21} &= -10.9254, \quad a_{22} = 0.218246, \\ a_{23} &= 0.140565, \quad a_{31} = 1.74146, \\ a_{32} &= 0.122687, \quad a_{41} = -1.86417, \\ a_{51} &= -0.128556, \quad b_{11} = -0.0611095; \end{aligned}$$

$$\begin{aligned} \alpha &= 0.59797; \quad E_{rc} \equiv E_{min}/|a_{21}| = 5.702 \times 10^{-6}; \\ \beta &= 2\alpha/F^2 = 0.76540, \end{aligned} \quad (40)$$

Here, we note that for greater wave height, it takes more a_{1n} (here up to $N = 13$) terms than all the previous cases to gain accuracy. While the error E_{min} is slightly greater than before, the relative error E_{rc} here is nevertheless still of $O(10^{-6})$ due to the larger values reached by some coefficients. In passing, we point out that some intermediate terms like $a_{19}, a_{1,11}, a_{1,13}$, etc. are left out by their smallness from optimization, and the term with b_{11} is admitted for the first time for this sufficiently high medium waves by optimization. These are the general trend found for Froude number greater than $F = 1.25$.

Thus, for higher extreme solitary waves, solutions of comparable high accuracy are still feasible by applying UIFE-Method-I. However, the trend demonstrated by the above example indicates that more IC-modes are needed, whilst iterative operations for optimization with thirty or more component functions simply become lengthy and inefficient. We therefore turn to UIFE-Method-II which is developed for automatic iterative computation of solutions for such cases to achieve higher accuracies.

4.5 Accurate solutions by UIFE-Method-II

The UIFE-Method-II was developed earlier in this study when this new theory was first conceived. A solution structure closely analogous to that for Method-I was adopted to establish a numerical code along a classical approach for computation of solutions; it however lacks such versatility as that open to Method-I for selecting the IC-modes with stepwise optimization by principle (ii). Otherwise, it has advantages in other aspects, the first being its capacity of gaining higher accuracy. Further, Method-II complements Method-I to facilitate computation of almost-highest waves owing to its convenience gained from using $\beta (= 1 - q_c^2 = 2\alpha/F^2)$ as a free parameter by virtue of the fact that $\alpha(\beta)$ is monotonic over $0 \leq \beta \leq 1$ whereas $\alpha(F)$ is multivalued for extreme waves. Thus, from the Bernoulli equation (5), $(1 - q^2) = 2\eta(\sigma)/F^2 = \beta\eta(\sigma)/\eta(\pi)$, which we rewrite, for convenience of computation by Method-II, in the form

$$G_2(\sigma) \equiv \frac{1}{q^2} (1 - \beta \frac{\eta(\sigma)}{\eta(\pi)}) - 1 = 0, \quad (41)$$

where $\eta(\sigma)$ is given by (17) and $\eta(\pi) = \alpha$, the wave height. The formulation is thus complete with (15)–(16) as the two kinematic conditions in addition.

For w , scaled by wave velocity c , we assume its UIF-expansion as

$$w^{-1}(\zeta) = q^{-1} e^{i\theta} = 1 + \sum_{m=1}^M \sum_{n=0}^N a_{mn} \left(\frac{1-\zeta}{2}\right)^{2m+n} \zeta^n, \quad (\text{for } 0 < \beta < 1), \tag{42}$$

for waves of height less than the highest, whereas for the highest wave, $\beta = 1$,

$$\begin{aligned} w^{-1}(\zeta) &\left(\frac{1+\zeta}{2}\right)^{1/3} \\ &= 1 - \frac{1-\zeta}{6} + \sum_{m=1}^M \sum_{n=0}^N \sum_{k=0}^K a_{mnk} \left(\frac{1-\zeta}{2}\right)^{2m+n} \\ &\quad \times \left(\frac{1+\zeta}{2}\right)^{2nv} \zeta^k, \end{aligned} \tag{43}$$

while condition (25) pertaining to the above expression for the highest wave becomes

$$H \equiv 1 - 3 \sum_{m=1}^M \sum_{k=0}^K (-1)^k a_{m,0,k} + \log\left(\frac{\pi}{3} F_{hst}^2\right) = 0. \tag{44}$$

These UIF-expansions for $w^{-1}(\zeta)$ are closely analogous to that for $\omega(\zeta)$ in (28) and (32); their expressions on the wave surface are very similar, and hence are omitted here.

The problem, by principle (ii), is then to minimize the mean-square-error functional

$$E^2(a_{mn}, \beta) = \int_0^\pi G_2^2(q(\sigma), \eta(\sigma), \sigma; a_{mn}, \beta) d\sigma, \quad (0 < \beta < 1), \tag{45}$$

with q and G_2 given by (41)–(42), η by (17), and β given, whereas for the highest wave, $\beta = 1$, we minimize E^2 given by

$$E^2(a_{mnk}, F_{hst}) = \int_0^\pi G_2^2(q(\sigma), \eta(\sigma), \sigma; a_{mnk}, \beta = 1) d\sigma + \lambda H, \tag{46}$$

in which $q(\sigma)$ of G_2 is given by (43) and (41) (with $\beta = 1$), and λ is a Lagrangian multiplier.

To obtain solutions with high accuracy, we solve the minimization problem with a sufficiently large number of IC-modes a_{mn} 's and b_{mn} 's along the following scheme. First, for all waves save the highest, $0 < \beta < 1$, starting with a given β also determines the velocity q_c at the crest (see (12)) plus the ratio α/F^2 , so that one of the mode coefficient and one parameter can be eliminated. After this we count all the unknowns including the remaining coefficients of a_{mn} ($m = 1, 2, \dots, M$; $n = 0, 1, \dots, N$) so that we can make a complete list of unknowns which we call the vector $\mathbf{x} = (x_1, x_2, \dots, x_L)$, of dimension L . In this vector space, the minimum of E^2 must satisfy

$$\frac{\partial E^2}{\partial x_i} = 0 \quad (i = 1, 2, \dots, L).$$

Table 1 Variations of $\alpha(\beta)$ and $F(\beta)$ — by UIF- Method-II

β	α	F	E_{max}	VdB/Miloh
0.300000	0.111033	1.053723	2.02×10^{-6}	
0.300000	0.176148	1.083661	1.6×10^{-7}	
0.351018	0.21228426	1.09978834	1.2×10^{-8}	
0.458885	0.2960185	1.1358535	4×10^{-7}	
0.498917	0.3298574	1.1499108		
0.584250	0.40743022	1.18097922	3.8×10^{-8}	
0.634846	0.4570637	1.1999668		
0.753499	0.58369035	1.24470064	3.0×10^{-8}	
0.7818	0.61558	1.2549		
0.840000	0.68193652	1.27422855	7×10^{-9}	
0.853316	0.69698819	1.27812334	4.9×10^{-8}	
0.878825	0.7253045	1.2847658	1.8×10^{-6}	1.28472
0.900000	0.7479485	1.2892276	2.7×10^{-6}	
0.910000	0.75824470	1.29091908	2.45×10^{-6}	
0.940277	0.7872063	1.2939914	6.5×10^{-6}	1.29395
0.948000	0.7939264	1.2941987	3.8×10^{-6}	
0.949000	0.7947741	1.294206978	2.1×10^{-8}	
0.950000	0.7956161	1.294210710	3.15×10^{-8}	
0.950300	0.7958677	1.294210973	1.84×10^{-8}	
0.950500	0.7960352	1.294210928	2.01×10^{-8}	
0.950700	0.79620238	1.294210706	2.18×10^{-8}	
0.951000	0.7964528	1.294210043	2.52×10^{-8}	
0.951600	0.79695221	1.294207527	3.13×10^{-8}	
0.952000	0.7972840	1.29420496	3.52×10^{-8}	
0.955000	0.7997435	1.2941621	2.2×10^{-5}	
0.967600	0.80953812	1.29355745	1.0×10^{-7}	
0.970108	0.8113862	1.2933581	1.1×10^{-6}	1.29332
0.985600	0.8222791	1.2917375	8.4×10^{-5}	
0.988000	0.82395	1.29147	4×10^{-5}	1.29144
0.990000	0.82535649	1.291273345	6.17×10^{-7}	
0.996400	0.83016026	1.290859899	1.15×10^{-6}	
0.997500	0.83106436	1.290850281	4.22×10^{-7}	
0.998400	0.83182712	1.290860312	7.64×10^{-7}	
0.999100	0.83243774	1.290881565	6.1×10^{-5}	
1.000000	0.83319905	1.290890430	2×10^{-7}	1.29091

We solve this set of L nonlinear equations in $\{x_i\}$ by applying Newton's method, for which we operate with the matrix equation

$$A_{ij} \Delta x_j = b_i \quad (i = 1, 2, \dots, L),$$

where $A_{ij} = (\partial^2 E^2 / \partial x_i \partial x_j)_0$, $b_i = (\partial E^2 / \partial x_i)_0$, the sub-index 0 denoting the values evaluated at $x_{i,0}$ in the iteration variables $x_i = x_{i,0} + \Delta x_i$ used at each preceding step for repeated corrections of Δx_i until the residues become small enough to fall within an error bound.

For the highest wave, $\beta = 1$, we apply Method-II to (46) instead, with the undetermined multiplier as a new unknown but otherwise following the same procedure. In practice for all cases, the initial estimates can assume an early stage solution of Method-I, or a solution by some lower-order theory with a relatively small number of L unknowns and let L be increased with the iteration process to reduce the local and global errors. In this manner, computations have been carried out to produce exact solutions for a set of values of β , especially concentrated about the highest and fastest solitary waves. The final results on the speed-amplitude relations are given jointly with those by Method-I in Table 1.

Here E_{max} stands for the maximum local error in G_2 of (41), and VdB/Miloh refers to comparisons with [24].

4.6 Graphical presentation of numerical solutions for solitary waves

The principal issues of significance in representing solitary waves are thought to cover three categories, (i) wave speed, (ii) geometric configuration of wave profile, and (iii) their integral properties, all as functions of wave height or an equivalent parameter, here alternatively taken in β . These characteristics have been derived from the exact solutions given in numerics jointly by our Method-I and Method-II, and are given below.

First, the data on wave speed are compiled in Fig. 5 as a function of wave height over the entire range $0 < \alpha = a/h \leq \alpha_{hst} = 0.8332$, in which the plotted dots denote the data relating amplitude and speed, and the full curve provides the values of $F(\alpha)$ given by a spline fit to the solution data. The range of the extreme waves ($0.68 < \alpha < 0.8832$) is magnified for exhibition in Fig. 6 with an eighth-degree polynomial curve fit to data. A still higher magnification of the neighborhood of the maximum wave speed is shown in Fig. 7 with a second-degree polynomial curve fit. From this fit, we find that the fastest wave has the maximum speed of

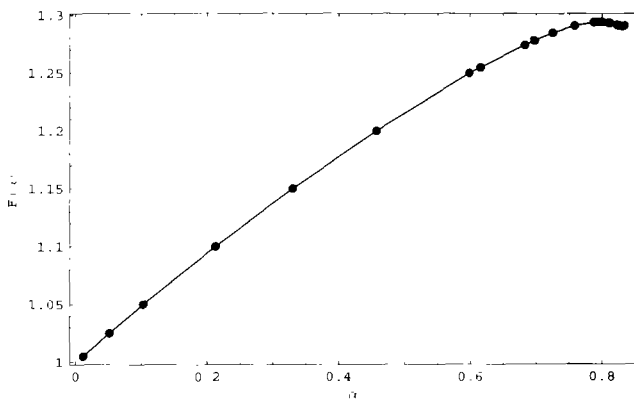


Fig. 5 Variation of wave speed $F(\alpha)$ as a function of wave height α over the entire range ($0 < \alpha < \alpha_{hst} = 0.8332$), shown with a spline fit to the solution data

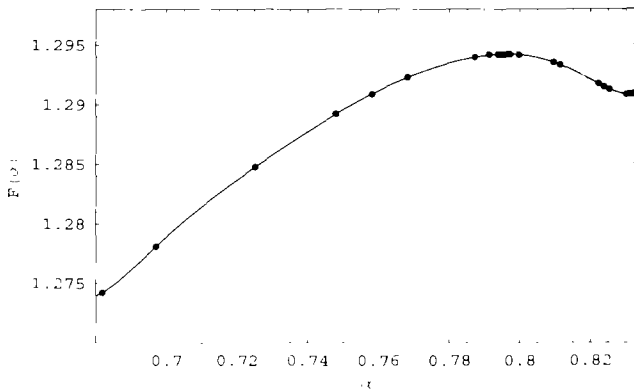


Fig. 6 Variation of wave speed $F(\alpha)$, magnified for extreme solitary waves over the range ($0.68 < \alpha < 0.8332$), shown with a 8th-degree polynomial curve fit to data

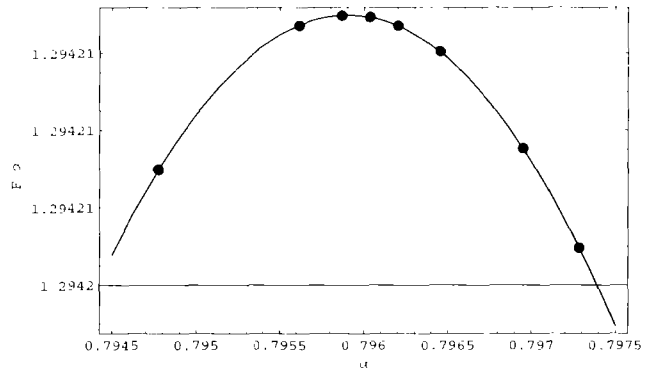


Fig. 7 Telescopic view of wave speed $F(\alpha)$ near the maximum $F = F_{hst} = 1.294211$ of the fastest solitary wave of height $\alpha_{fst} = 0.7959034$, shown with a second-degree curve fit

$F_{fst} = 1.294211$ and its height at $\alpha_{fst} = 0.7959034$, with accuracy up to $O(10^{-6})$ or higher.

Beyond the fastest wave, the amplitude-speed curve is found to reach a second extremum, which is a local minimum as exhibited with magnification in Fig. 8, from which we find the local minimum speed by a third-degree polynomial fit as $F_{min} = 1.29085$ for a wave of height $\alpha_{min} = 0.83106$. The curve finally proceeds with a very small positive slope in reaching the maximum height. Existence of the second extremum (a local minimum) has been found by [19] for speed and for some other integral properties.

Turning to the issue on wave profile, we first present in Fig. 9 four profiles for waves of height $\alpha = \alpha_{hst}$ (0.8331990), 0.822279, 0.811386, and 0.796952 (with speed F_{hst} (1.290890), 1.291738, 1.293358, 1.294208, respectively). The distant view of the four profile images superimposed here gives an overall impression that they are nearly coincident save for a small neighborhood of the wave crest. A telescopic close-up view of the wave crests given in an inset of Fig. 9 however distinguishes between the four crests, revealing that the slightly lower waves intersect the highest

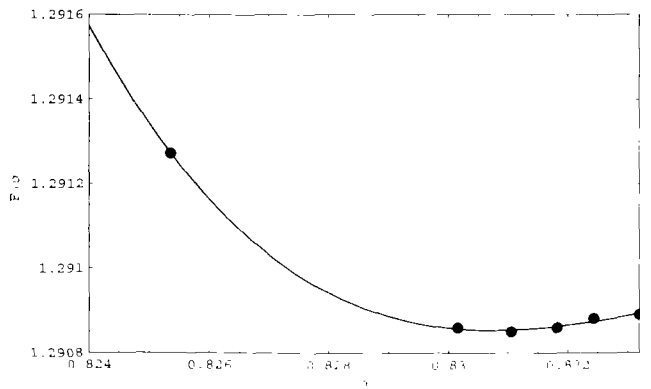


Fig. 8 Variation of wave speed $F(\alpha)$ near its local minimum at $F_{min} = 1.29085$ for a wave of height $\alpha_{min} = 0.83106$, shown with a 3rd-degree polynomial curve fit to data

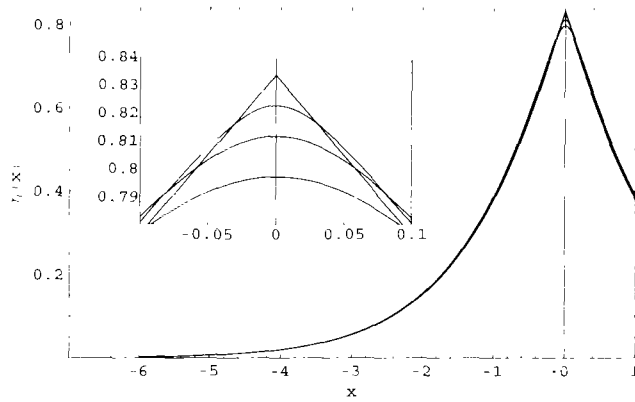


Fig. 9 Distant and close-up views of four wave profiles given by UIFE-Method-I and -II for extreme solitary waves of height $\alpha = \alpha_{hst}$ (0.8331990), 0.822279, 0.811386, and 0.796952, with corresponding speed F_{hst} (1.290890), 1.291738, 1.293358, 1.294208. Note that the last three waves are successively lower in height but all increasingly faster than the highest wave, the last being almost exactly the fastest one ($\alpha_{fst} = 0.7959034$, $F_{fst} = 1.294211$)

to become somewhat broader beyond the cross-over, with the point of intersection moving closer to the corner of the highest wave as the wave increases both in height and curvature at the crest. This also implies that the approaching process to the corner crest is one strongly singular. We further point out that the three waves with a round crest are successively lower in height but all increasingly faster in speed than the highest wave, the last being almost exactly the fastest one.

Figure 10 shows five profiles for waves of height $\alpha = \alpha_{hst}$, 0.758245, 0.583690, 0.407430, 0.212284, with the corresponding speed $F = F_{hst}$, 1.29092, 1.24470, 1.18098, 1.09979, respectively. For waves of decreasing height, they become broader and slightly greater in local surface elevation beyond crossing over the higher waves, noticeably with such gains appearing increasingly more expansive for low, and very low waves.

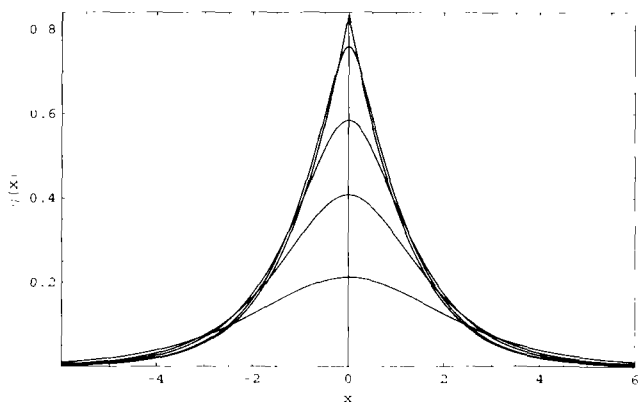


Fig. 10 Wave profiles evaluated by UIFE-Method-I and -II for five solitary waves of height $\alpha = \alpha_{hst} = 0.8331990$ (the highest), 0.758245, 0.583690, 0.407430, 0.212284, corresponding with speed $F = F_{hst} = 1.2908904$, 1.29092, 1.24470, 1.18098, 1.09979, respectively. Note that the second wave is lower in height but faster in speed than the highest wave; and it is already lower than the fastest wave

5 Integral properties of solitary waves

The integral properties of solitary waves, including the excess mass, total momentum, kinetic and potential energy, and the net circulation, have been studied by [6, 15, 19, 25] and others for their importance to wave dynamics, notably to wave breaking in shallow water. In this respect, the existing exact relations between these integral properties initiated by [31, 32] and extended by [25] and others have played their useful roles in providing results with high accuracy. There it has been found that speed F , the mass, momentum, and energies all separately attain not only a maximum for waves at a height less than the maximum amplitude ([6]), but also a second extremum (local minimum) for waves at a height even closer to the maximum amplitude ([19]). On the other hand, these properties are not known to have been studied for solitary waves of low and very low heights. We now take up this entire issue for study.

The excess mass, M , kinetic and potential energy, E_k and E_p , and net circulation, Γ , are defined by

$$M = \int \eta \, dx, \quad E_k = \frac{F^2}{2} \int \int_1^\eta \tilde{u} \cdot \tilde{u} \, dy \, dx, \\ E_p = \int \frac{\eta^2}{2} \, dx, \quad \Gamma = F \int \tilde{u} \cdot dx, \quad (47)$$

where $\tilde{u} = (u - 1, v) = \nabla \tilde{\phi}$ (with velocity potential $\tilde{\phi} = \phi - x$) is the flow velocity vector in the absolute frame of reference, and all the longitudinal integrals in x are over $(-\infty < x < \infty)$ except for Γ which assumes the sense of wave progression so that Γ is always positive definite. Here, M is scaled by ρh^2 , E_p and E_k by $\rho g h^3 = \rho h^2 c_0^2$, $c_0 = \sqrt{gh}$, and Γ by $h c_0$. The excess mass M can be evaluated either by integrating $\eta(x)$ over x or by

$$M = \int \eta \, dx = \int \eta \frac{dx}{ds} \frac{ds}{d\phi} \, d\phi \\ = F^2 \int_0^\tau (e^{-\tau} - e^\tau) \cos \theta \, d\phi(\sigma), \quad (48)$$

where the last step is by using (18), rendering the integral ready for quadrature in σ .

The momentum (or impulse), I , scaled by $h^2 c_0$, is defined as the volume integral of the perturbation velocity, $\tilde{u} = \partial \tilde{\phi} / \partial x = u - 1$, throughout the flow field; it is related to excess mass M by Starr's exact relation

$$I \equiv F \int \int_1^\eta (\tilde{u}) \, dy \, dx = FM. \quad (49)$$

We remark that I assumes the sense of the wave, hence is positive definite.

For the energy, the potential energy follows at once from another identity of Starr's,

$$E_p = (F^2 - 1)M/3. \quad (50)$$

Table 2 Variations of α , F , $F^2 - 1$, M , Γ , E_p and E_k as functions of β

β	α	F	$F^2 - 1$	M	Γ	E_p	E_k
0.022658	0.011443	1.00500	0.0100	0.248040	0.247637	0.0008289	0.0008255
0.098559	0.051774	1.02500	0.0506	0.532785	0.527898	0.0089908	0.0093314
0.186175	0.102629	1.05000	0.1025	0.767632	0.754351	0.0262274	0.0271228
0.351185	0.212467	1.10000	0.2100	1.135830	1.094135	0.0795080	0.0854027
0.498914	0.329907	1.15000	0.3225	1.444290	1.361129	0.1552620	0.1723930
0.634864	0.457102	1.20000	0.4400	1.714750	1.577508	0.2514970	0.2881170
0.765400	0.597971	1.25000	0.5625	1.944911	1.745225	0.3646700	0.4286930
0.853316	0.696988	1.27812	0.6336	2.024838	1.783307	0.4276453	0.5143476
0.910000	0.758245	1.29092	0.6665	2.032937	1.773780	0.4516319	0.5489400
0.952000	0.797284	1.29420	0.6750	2.005220	1.743529	0.4511517	0.5512650
0.970108	0.811390	1.29335	0.6728	1.986686	1.727307	0.4455311	0.5449277
0.985600	0.822278	1.29174	0.6686	1.972860	1.715525	0.4396728	0.5377085
1.000000	0.833199	1.29089	0.6662	1.969170	1.713828	0.4372420	0.5345360

For the kinetic energy E_k , we start from

$$\begin{aligned}
 \frac{2}{F^2} E_k &= \int \int_{-1}^{\eta} (\nabla \tilde{\phi})^2 dy dx = \oint \tilde{\phi} \frac{\partial \tilde{\phi}}{\partial n} ds \\
 &= - \oint \tilde{\phi} dy = \int \tilde{\phi} d\eta(x) = - \int_{-\infty}^{\infty} \eta d\tilde{\phi}(x) \\
 &= \int \eta(dx - d\phi) \\
 &= M - F^2 \int_0^{\pi} (1 - e^{-2\tau}) d\phi(\sigma), \quad (51)
 \end{aligned}$$

which follows first by applying the divergence theorem, with the outward normal derivative $\partial \tilde{\phi} / \partial n = -\partial y / \partial s$ taken counterclockwise along the boundary contour, then by integration by parts, next by making use of (18), and finally by quadrature in σ .

For the circulation Γ , we have from (49),

$$\begin{aligned}
 \Gamma &= F \int \nabla \tilde{\phi} \cdot dx = F \int d\tilde{\phi}(x) = F \int (d\phi - dx) \\
 &= 2F \int_0^{\pi} (1 - e^{\tau} \cos \theta) d\phi(\sigma), \quad (52)
 \end{aligned}$$

which is readily integrated. Alternatively, we have McConwan's identity,

$$2E_k = F(FM - \Gamma), \quad (53)$$

which we can use to determine Γ or for a check up with the previous formula for Γ .

Applying these formulas to the exact solutions, we have the results given in Table 2.

Variations of these integral properties as functions of β are shown graphically in Fig. 11, exhibited with curves given by a seventh-degree polynomial fit to data. Their general behavior as functions of a parameter called $\omega_2 (= 1 - F^2 q_c^2)$ by definition, in the present notation) has been discussed in detail by [12]. The behavior of these conserved integral quantities are found very similar in terms of β as in ω_2 , now with their relative errors updated by the present study, which is of $O(10^{-6})$ at $\beta = 1$ and comparable elsewhere of β . For $\beta \ll 1$, mass M and circulation Γ rise steeply from the origin, while α and $F^2 - 1$ increase linearly with $\alpha \simeq (F^2 - 1) = \beta/2$,

and both E_p and E_k grow proportional to β^2 . Of these integral variables, only wave height α is a monotonic function of β throughout $0 \leq \beta \leq 1$, whereas the other variables all have one local maximum with their values, derived from the polynomial fit, given by

$$\begin{aligned}
 (F^2 - 1)_{\max}(0.9568) &= 0.6745, & M_{\max}(0.8771) &= 2.038, \\
 \Gamma_{\max}(0.8550) &= 1.788, \\
 E_{p\max}(0.9352) &= 0.4520, \\
 E_{k\max}(0.9421) &= 0.5516. \quad (54)
 \end{aligned}$$

The advantage of having these conservation properties in precise values may afford a standard reference for further studies.

For comparison, we note that the present results given in Table 2 agree with those of Williams ([23], Table 5 giving only for the case $\beta = 1$ of the highest wave) up to four, down to three decimal places, whereas ours have errors (see (31)) no greater than 10^{-6} .

6 Discussions and conclusion

Summing up this work, we have seen Stokes's and other pioneers' contributions reflected, studied, and generalized to develop a new theory for solitary waves of all heights. The power, simplicity, and high accuracy of the new theory have been illustrated with examples. As this theoretical approach is new, issues of significance should merit an expository discussion on its salient and outstanding features.

First, at the foundation of this new theory, it is essential to find the precise intrinsic properties of the wave entity to construct a unified intrinsic functional expansion for a comprehensive and optimum representation of the solution under a specific premise (e.g. wave speed or wave height). To the importance in first establishing a comprehensive and optimum UIF-expansion we may give a counter example to the fact that the ignorance (in an early era) to the existence of the complementary branch-singularity in the solution for the highest solitary wave had unwittingly kept the computational studies (on the highest solitary wave prior to Grant, [28]) from achieving accuracy higher than the actually attained. Indeed, without admitting this complementary singularity, it would

have required some scores to hundreds of terms to reach the present level of accuracy, if attainable at all.

Conceptually speaking, we note that with the unified intrinsic functional expansion well established, and with the optimization carried out stepwise aptly in evaluating the exact solution, accurate solutions attained by this method can well return more sharply focused data on the underlying wave properties, shed new light on the initial concept about the wave problem (like constructing its *intrinsic* component (IC)-modes), and open new ways for further studies. For instance, in the solution (30) for the highest solitary wave, the twelve intrinsic modes optimally selected are seen evenly distributed among three groups (pertaining separately to the outskirt decay, to the branch singularity at the crest, and to the regular behavior in the inner flow field). In contrast, for the low wave of height $\alpha = 0.011$ at $F = 1.005$ of example 1-7, it also takes only twelve IC-modes for the solution, with however eleven modes in a_{m0} ($m = 1, \dots, M = 11$) for describing the outskirt attenuation, leaving only one mode of the first order, a_{11} , admitted by optimization to yield a solution, accurate to $O(10^{-7})$. These features of the solutions are so salient and definitive that such new data on the wave behavior should be regarded as the merits unique to this method, and so succulent and valuable that they can be used reliably to predict the behavior of neighboring waves by interpolation or extrapolation. On the contrary, had some arbitrary modes been admitted at will, it might then require taking many more

other modes (most likely in those bearing coefficients b_{mm} in (28) or (32)) to reach comparable accuracy, if successful at all. On this note, this new theory may be said to have merits in simplicity in implementation, and in richness in returning information on problems solved.

Mathematically speaking, this new method appears rather preliminary in status, but simple and proficient in practical application, and highly promising for future development. Aside from the existing mathematical resources available for finding the desired IC-modes, new studies are in need for finding definitive ways of construction of solution and for error estimation or proof. In this aspect, it differs from the other approaches dependent on using series expansions or integral equations involving use of scores to hundreds of grid points for lengthy computation and the need for considering the convergence for their results.

Furthermore, we point out a new exposition that the class of very low solitary waves appears to promise more contents of richness to attract new interest and new devotion to finding effective newer methods of solution. On this issue, it might be natural, by intuition, to push forward a contention that for very, very low solitary waves, a lower-order theory, such as the KdV model of the first order should suffice for their accurate description. The total lack of a sound physical ground in such a naive concept can be easily seen by noticing the fact that solitary waves of infinitesimal height are also exceedingly long in length. In this respect, we propose to call the waves with height $\alpha \leq 10^{-2}$ dwarf solitary waves as a new field, which includes the earthquake-produced tsunamis progressing in the open ocean with a height commonly estimated to be of order $\alpha = O(10^{-4})$.

In conclusion, we wish to say that the new approach introduced here is but a beginning for further studies on wave problems involving fully nonlinear and fully dispersive effects as well as on similar physical phenomena. It is by and large held for continuing studies and very much open for creative ideas and academic interaction.

Acknowledgements We wish to thank Dr. Xinlong Wang of Nanjing University for enlightening discussions. We are further very appreciative for the encouraging sponsorship from the American-Chinese Scholarship Foundation and for the partial support by U.S. NASA Grant NAGS-5338 and NASA JPL Grant JPL-000078.

References

1. Stokes, G.G.: On the theory of oscillatory waves. Appendix B. *Math. and Phys. Pap.* **1**, p. 197–229, p. 314–326 (1880). Cambridge Univ. Press
2. Boussinesq, J.: Théorie de l'intumescence liquide appelée onde solitaire ou de translation se propageant dans un canal rectangulaire. *C.R. Acad. Sci. Paris* **72**, 755–759 (1871)
3. Rayleigh, Lord: On waves. *Phil. Mag.* **1**, 257–279 (1876); Reprinted in *Scientific papers*, vol. **1**, 251–271
4. Korteweg, D.J., de Vries, G.: On the change of form of long waves advancing in a rectangular channel, and on a new type of long stationary waves. *Philos. Mag.* **39**, 422–443 (1895)
5. Fenton, J.: A ninth-order solution for the solitary wave. *J. Fluid Mech.* **53**(2), 257–271 (1972)

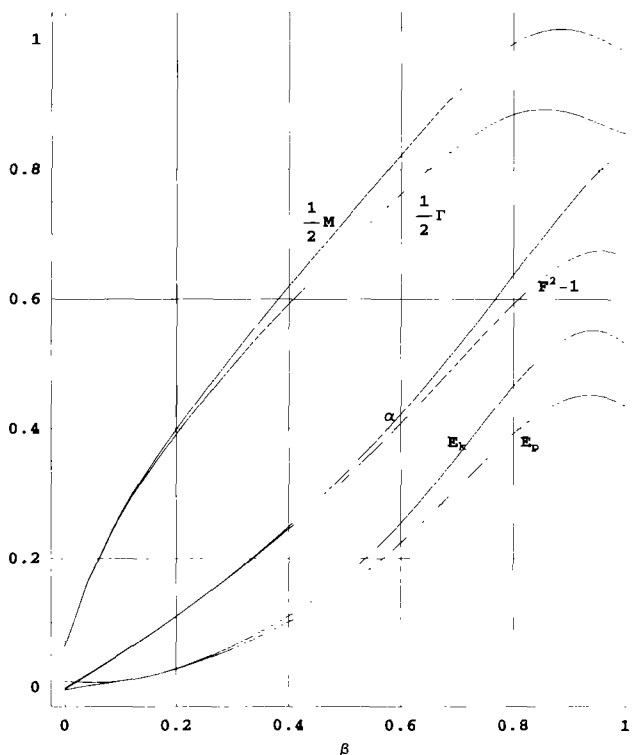


Fig. 11 Variations of mass M , circulation Γ , wave height α , $F^2 - 1$, kinetic energy E_k , and potential energy E_p as functions of the *proportional amplitude parameter* β

6. Longuet-Higgins, M.S., Fenton, J.: On the mass, momentum, energy and circulation of a solitary wave. II, *Proc. R. Soc. Lond. A* **340**, 471–493 (1974)
7. Qu, W.-D.: Studies on nonlinear dispersive water waves, PhD thesis, California Institute of Technology, 2000
8. Wehausen, J.V., Laitone, E.V.: Surface waves. In: Flügge, S., Truesdell, C. (eds.), *Handbuch der Physik*, Vol IX Springer Verlag, 1960
9. Miles, J.W.: Solitary waves. *Ann. Rev. Fluid Mech.* **12**, 11–23 (1980)
10. Longuet-Higgins, M.S., Fox, M.J.H.: Asymptotic theory for the almost-highest solitary wave. *J. Fluid Mech.* **317**, 1–19 (1996)
11. Wu, T.Y.: A unified theory for modeling water waves. *Adv. Appl. Mech.* **37**, 1–88 (2000)
12. Nekrasov, A.I.: On waves of permanent type. I. *Izv. Ivanovo-Voznesensk. Politekh. Inst.* **3**, 52–65 (1921)
13. Milne-Thomson, L.M.: An exact integral equation for the solitary wave. *Rev. Roum. Sci. Techn. -Mec. Appl.* **9**, 1189–1194 (1964)
14. Milne-Thomson, L.M.: *Theoretical Hydrodynamics*, 5th edn. London: Macmillan, 1968
15. Byatt-Smith, J.G.B.: An integral equation for unsteady surface waves and a comment on the Boussinesq equation. *J. Fluid Mech.* **49**, 625–633 (1971)
16. Byatt-Smith, J.G.B., Longuet-Higgins, M.S.: On the speed and profile of steep solitary waves. *Proc. R. Soc. Lond. A* **350**, 175–189 (1976)
17. Friedrichs, K.O., Hyers, D.H.: The existence of solitary waves. *Commun. Pure Appl. Math.* **7**, 517–550 (1954)
18. Tanaka, M.: The stability of steep gravity waves. *J. Fluid Mech.* **156**, 281–289 (1985)
19. Tanaka, M.: The stability of solitary waves. *Phys. Fluids* **29**(3), 650–655 (1986)
20. Yamada, H.: On the highest solitary wave. *Reports of Research Institute for Applied Mechanics, Kyushu University*, **V**(14), 53–67 (1957)
21. Lenau, C.W.: The solitary wave of maximum amplitude. *J. Fluid Mech.* **26**(2), 309–320 (1966)
22. Witting, J.: On the highest and other solitary waves. *SIAM J. Appl. Math.* **28**(3), 700–719 (1975)
23. Williams, J.M.: Limiting gravity waves in water of finite depth. *Philos. Trans. Roy. Soc. Lond. A* **302**, 139–188 (1981)
24. Vanden-Broeck, J.-M., Miloh, T.: Computations of steep gravity waves by a refinement of Davies-Tulin's approximation. *SIAM J. Appl. Math.* **55**(4), 892–903 (1995)
25. Longuet-Higgins, M.S.: On the mass, momentum, energy and circulation of a solitary wave. *Proc. R. Soc. Lond. A* **337**, 1–13 (1974)
26. Longuet-Higgins, M.S., Fox, M.J.H.: Theory of the almost-highest wave: the inner solution. *J. Fluid Mech.* **80**(4), 721–741 (1977)
27. Longuet-Higgins, M.S., Fox, M.J.H.: Theory of the almost-highest wave. Part 2. Matching and analytic extension. *J. Fluid Mech.* **85**(4), 769–786 (1978)
28. Grant, M.A.: The singularity at the crest of a finite amplitude progressive Stokes waves. *J. Fluid Mech.* **59**, 257–262 (1973)
29. Fox, M.J.H.: Nonlinear effects in surface gravity waves. Ph.D. thesis, Cambridge University, 1977
30. Hunter, J.K., Vanden-Broeck, J.-M.: Accurate computations for steep solitary waves. *J. Fluid Mech.* **136**, 63–71 (1983)
31. Starr, V.P.: Momentum and energy integrals for gravity waves of finite height. *J. Marine Res.* **6**, 175–193 (1947)
32. McCowan, J.: On the solitary wave. *Phil. Mag.* (5)**32**, 45–58 (1891)